

Measurements of the Multiple Coulomb Scattering of Muons by MICE

Ryan Bayes on behalf of the MICE collaboration

School of Physics and Astronomy, University of Glasgow, University Avenue, Glasgow, U.K., G12 8QQ



Multiple coulomb scattering is a well known electromagnetic phenomenon experienced by charged particles traversing materials. However, from recent measurements by the MuScat experiment it is known that the available simulation codes, specifically GEANT4, overestimate the scattering of muons in low Z materials. This is of particular interest to the Muon Ionization Cooling Experiment (MICE) which has the goal of measuring the reduction of muon beam emittance induced by energy loss in low Z absorbers. Multiple scattering induces positive changes in the emittance in contrast to the reduction due to ionization energy loss. It therefore is essential that MICE measures multiple scattering for its absorber materials; lithium hydride and liquid hydrogen; and validate the known simulations of multiple scattering against data. MICE took data with magnetic fields off suitable for multiple scattering measurements in the spring of 2016. The results of these measurements and comparison of the data to available simulations will be discussed. Further measurements of multiple scattering with magnetic fields on are planned and the impact of the increased angular acceptance on the resulting measurements will also be discussed.

1 Introduction

The Muon Ionization Cooling Experiment (MICE) is tasked with determining the viability of ionization cooling for the purpose of conditioning muon beams¹. Ionization cooling is a result of electromagnetic interactions of the beam particles as they pass through an absorber material. This process is of particular interest to the development of neutrino factories² and muon colliders³ as it can act on a beam well within the muon lifetime. The extent of particle beams is expressed as a normalized emittance ϵ_n which is the fourth root of the determinant of the covariance matrix of the beam in the transverse position and momentum divided by the particle mass. Channel performance is given by

$$\frac{d\epsilon_n}{dz} \approx -\frac{\epsilon}{p_\mu\beta} \left\langle \frac{dE_\mu}{dz} \right\rangle + \frac{\beta_\perp p_\mu}{2m} \frac{d\theta_0^2}{dz} \quad (1)$$

where the first term represents the reduction in the emittance of the beam due to energy loss in and the second term increases the beam emittance due to multiple scattering quantified by the RMS width θ_0 for a beam with a transverse momentum envelop characterized by β_\perp , a momentum p_μ and a relativistic velocity β . Rossi and Greisen derived the scattering width⁴

$$\theta_0 \approx \frac{14 \text{ MeV}/c}{p_\mu\beta} \sqrt{\frac{z}{X_0}} \quad (2)$$

where X_0 is the radiation length of the material. Simulations of scattering by GEANT4, which uses a Legendre polynomial expansion to describe the scattering distribution were found to disagree significantly with the measurements for low Z materials made by the MuScat experiment⁵. It is important for MICE to measure the scattering distributions of muons in low Z materials in data to validate the emittance reduction predictions made by simulation.

When passing through matter, charged particles scatter due to interactions with (screened) nuclei and atomic electrons. The respective single scattering cross-sections are in the ratio Z^2

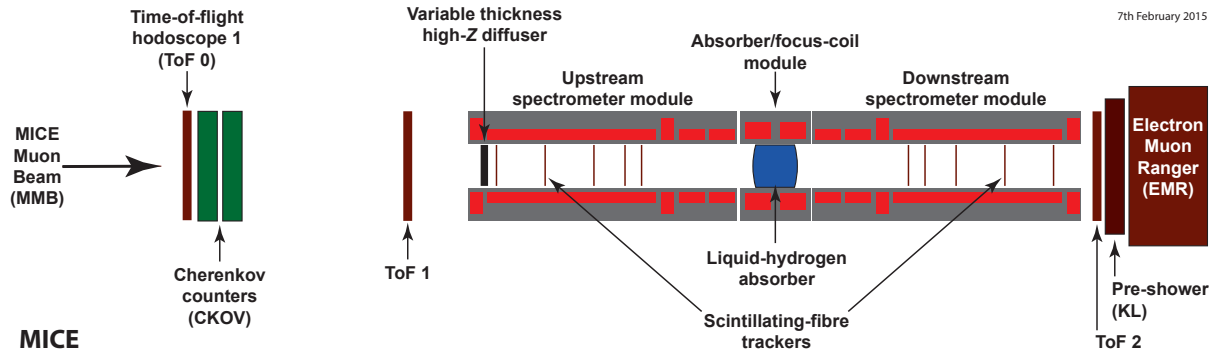


Figure 1: Schematic representation of the as built MICE channel.

to Z . The well known distribution for multiple scattering derived by Molière assumed scattering from screened nuclei alone; it was later modified by Bethe to include the scattering by electrons with the *ansatz* $Z^2 \rightarrow Z(Z + 1)$. It is found⁵ that neither the modified or unmodified Molière distribution adequately describes scattering in low Z materials, especially liquid hydrogen. The derivation of the multiple scattering distribution from the single scattering cross-sections is mathematically complicated and ultimately requires a numerical integration. An alternative approach is to use a bottom up, 'atomistic', Monte Carlo integration, as described by Carlisle⁶ which uses the screened nucleus cross-section and a similar cross-section for scattering by electrons. The MICE data presented in this paper will be compared with the results of such a simulation and the predictions of Geant4.

2 MICE Data Collection

MICE uses a low rate beam of muon and pion beams to characterize the behaviour of muons in the channel using single particle events. The MICE measurements are conducted in a channel consisting of a sequence of three superconducting magnets instrumented by a system of detectors that measures the paths of particles through the channel using the 10 tracker stations, and determines the particle identity using a set of time of flight (TOF) detectors, a pair of threshold Cherenkov detectors, a lead shower calorimeter, and a totally active scintillating detector. A schematic representation of the MICE experiment is shown in Fig.1. The absorber material is contained in the central solenoid, which is called the absorber focus coil. The tracker stations are contained in the spectrometer modules and are arranged symmetrically about the absorber. The tracker stations provide the track angles based on position measurements with a $490 \mu\text{m}$ resolution measurement yielding a 0.5 mrad angular resolution. The TOF measurements were used to select muon tracks from the collected sample based on the time difference between stations zero and one.

Data were collected in February and March 2016 using six different configurations with the solenoid magnetic fields off. Three different beam settings with modes at 172, 200, and 240 MeV/c were considered with an empty AFC and with a 6.5 cm lithium hydride disk installed in the AFC. A summary of the data collected is shown in Table 1a. The empty AFC provides a baseline measurement of the scattering in the channel in absence of the absorber encompassing tracker resolution and scattering from vacuum windows in the channel. The lithium hydride disk had a composition of 81% ${}^6\text{Li}$, 4% ${}^7\text{Li}$, 14% ${}^1\text{H}$ with some trace amounts of Carbon, Oxygen and Calcium. The simulation has confirmed that the measurement is insensitive to the precise composition of the LiH disk.

Table 1: Data used for the MCS analysis and the time of flight selection applied.

(a) Data collected by MICE in ISIS user cycle 2015-4.

State	TOF1	TOF2
Empty 172 MeV/c, Muon	624,577	94,722
Empty 200 MeV/c, Muon	384,909	56,314
Empty 240 MeV/c, Muon	314,739	62,546
LiH 172 MeV/c, Muon	1,282,488	174,405
LiH 200 MeV/c, Muon	1,223,560	177,460
LiH 240 MeV/c, Muon	1,239,827	232,982

(b) Time of flight selections for the difference between stations 0 and 1.

Beam Setting	lower limit (ns)	upper limit (ns)
172 MeV/c	28.7	28.9
200 MeV/c	27.7	27.9
240 MeV/c	27.2	27.4

3 Analysis

The analysis of the data starts with a simple selection of events that trigger TOF station 1. Such events must produce a straight trajectory in the upstream tracker stations. If that trajectory can be projected to a radial position greater than 150 mm from the centre of downstream tracker station 0 assuming that the projection scatters radially outward by 10 mrad, the event is rejected. Multiple scattering is a momentum dependent quantity, so a time of flight selection is applied to the events to narrow the momentum to be consistent with the generated scattering models. This selection is different for each of the muon beams generated as shown in Table 1b. Events which do not produce trajectories in the downstream tracker stations are counted to maintain the normalization condition for the scattering probability distributions. The measured projected scattering angles are

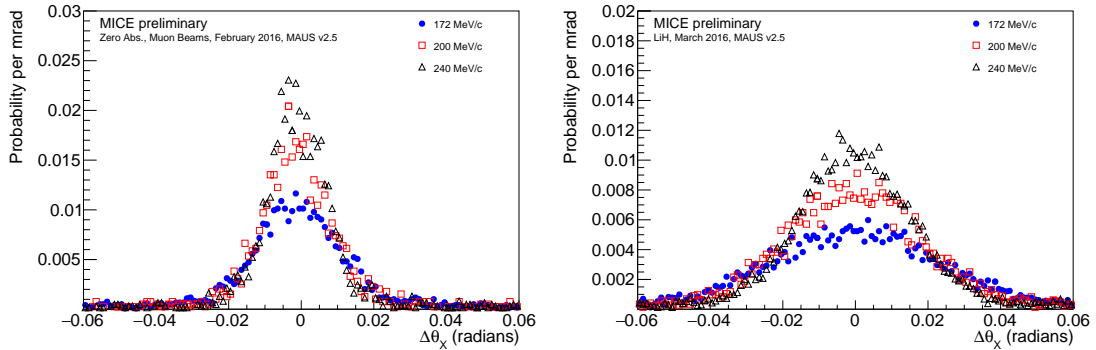
$$\Delta\theta_X = \arctan y'_{US} - \arctan y'_{DS}, \quad (3)$$

$$\Delta\theta_Y = \arctan x'_{US} - \arctan x'_{DS} \quad (4)$$

where $x' = dx/dz$ and $y' = dy/dz$. The 3D space angle of the muon across the absorber is

$$\theta_{Scatt} = \arccos \left(\frac{1 + x'_{US}x'_{DS} + y'_{US}y'_{DS}}{\sqrt{1 + (x'_{US})^2 + (y'_{US})^2} \sqrt{1 + (x'_{DS})^2 + (y'_{DS})^2}} \right) \approx \sqrt{\Delta\theta_X^2 + \Delta\theta_Y^2}. \quad (5)$$

The scattering distributions projected on the Y-Z plane for the three beam settings with no absorber are shown in Fig.2a and with the lithium hydride absorber are shown in Fig.2b. There is considerable scattering in muon channel from vacuum windows, even in the empty channel. To use the model distributions for model evaluation, scattering measured with the absorber in



(a) Scattering in channel without absorber.

(b) Scattering in channel with LiH Disk.

Figure 2: Multiple scattering distributions at the three different nominal beam momenta.

place must be compared to the convolution of the empty channel scattering distributions with the distribution of scattering in the absorber.

To compare the scattering data with the simulation a simple convolution between the empty channel data and the simulated scattering in LiH is made. The convolution is done by adding a random angle from the model of the projected scattering distribution to the downstream track angle measured from the no absorber data. This addition is done 10 times for every no absorber event to reduce sensitivity to statistical fluctuations. The convolved distribution can be compared to the selected data using χ^2 .

Tests of the models of MCS were conducted by defining a χ^2 with 100 degrees of freedom between the θ_{Scatt} distribution for the three collected data sets and the corresponding convolved data sets;

$$\chi^2 = \sum_{i=1}^{100} \frac{(n_{data}(\theta_i) - n_{conv.}(\theta_i))^2}{n_{data}(\theta_i) + n_{conv.}(\theta_i)}. \quad (6)$$

The preliminary mean 3D space angles for the measured data and the convolved distributions using the GEANT4 simulation and the Carlisle Cobb (CC) simulation for LiH are shown in Table 2, together with the χ^2 calculated between the data and convolved distributions. Preliminary results indicate a better match between the data to the Carlisle model for the described data selection in comparison to the GEANT simulation. These results are sensitive to systematic effects, the evaluation of which is in progress.

Deconvolution of the LiH scattering distribution from the measured scattering is a non-trivial procedure. For this analysis a deconvolution procedure is used that relies on Bayes' theorem to predict the scattering in the absorber material alone⁷. The algorithm to accomplish this is contained in the RooUnfold package⁸. This method uses the simulation in conjunction with the no absorber scattering data to produce a conditional probability, $P(\theta_j^{rec}|\theta_i^{abs})$ that a particle is measured at a particular angle θ_j^{rec} given a true scattering angle in the absorber material θ_i^{abs} . Application of Bayes' theorem then yields a conditional probability that may be used to provide an estimate of the number of events at θ_i^{abs} , given a number of events $n(\theta_j^{rec})$,

$$n(\theta_i^{abs}) = \sum_{j=1}^{n_E} n(\theta_j^{rec}) P(\theta_i^{abs}|\theta_j^{rec}). \quad (7)$$

This measure is iterated 10 times, updating the prior probability with $P_0(\theta_i^{abs}) = n(\theta_i^{abs}) / \sum_i n(\theta_i^{abs})$ used in the Bayes expansion of $P(\theta_i^{abs}|\theta_j^{rec})$ to better approximate the true distribution.

The measurements of scattering in lithium hydride is shown in Table 3. The widths of the projection angle, θ_X and θ_Y , are taken from a Gaussian fit for angles less than 0.04 radians while the mean of the 3D scattering angle is also shown. The deconvolution using both models have been completed and the results are more similar to each other than they are to the reference models. Again the scattering width is more consistent with the Carlisle Cobb implementation for the event selection described above.

4 Future Prospects

Consideration of the systematic effects in this measurement is ongoing so the specific results are not quoted here but the leading considerations should be discussed. The thickness of the

Table 2: Preliminary measurements of the mean 3D space angles after event selection.

P	$\langle \theta_{Scatt}^{meas} \rangle$ (mrad)	$\langle \theta_{Scatt}^{conv} \rangle_{G4}$	χ^2	$\langle \theta_{Scatt}^{conv} \rangle_{CC}$	χ^2
172	41.4 ± 0.4	37.2 ± 0.1	259.0	38.6 ± 0.1	149.3
200	36.4 ± 0.5	34.6 ± 0.2	225.9	32.8 ± 0.2	104.0
240	32.1 ± 0.4	30.1 ± 0.2	197.5	29.1 ± 0.1	102.7

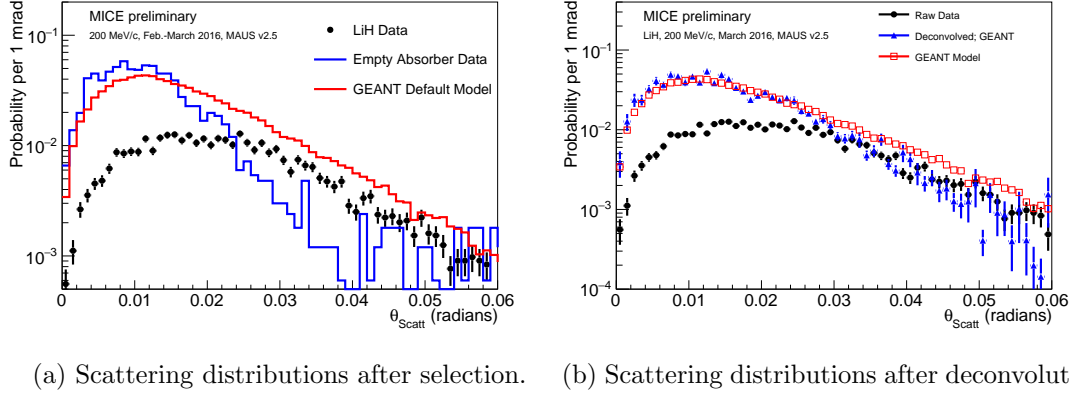


Figure 3: Distributions of the θ_{Scatt} illustrating the operation of the analysis procedures.

absorber is an obvious uncertainty in the scattering distribution since the width goes as the square root of the absorber thickness multiplied by the density of the absorber. Measurements of the LiH absorber mass and dimensions yield a density of 0.694 ± 0.003 g/cm³ and a 0.254 mm uncertainty for the absorber thickness. Changes in the measurement of the scattering distributions induced by variations in the absorber thickness are modelled by multiplying the widths of the scattering distribution used in the convolution with the empty AFC data by a factor consistent with a 3% density increase.

A significant systematic uncertainty is due to the TOF selection criteria which directly impacts the momentum range of the particles used in the scattering measurement. The scale is set by the 60 ps resolution of the time of flight measurements. To exaggerate the effect of particles incorrectly appearing inside or outside of the 200 ps selection window, the TOF selection window is offset by ± 400 ps and the difference in the measured scattering width, scaled by a factor of 60 ps/800 ps, is treated as the systematic uncertainty.

Other systematic contributions include uncertainties in the alignment. The alignment of the MICE trackers is characterized by four parameters defining offsets, with an uncertainty of 0.2 mm, and angles, with an uncertainty of 0.07 mrad in the X-Z and Y-Z planes; the z position of the tracker and rotations about the z axis are not accessible to the alignment. The alignment of the upstream tracker is independent of the downstream detector inflating the total number of parameters to eight. To assess the effect on the MCS widths, run a number of pseudo experiments have been run which vary the values of all of the alignment parameters within the errors. The uncertainties in the scattering width is extracted from the distributions of the

Table 3: Preliminary scattering widths measured from lithium hydride after deconvolution.

p	Angle	σ_{G4}^{meas} (mrad)	σ_{CC}^{meas} (mrad)	σ_{G4}^{model} (mrad)	σ_{CC}^{model} (mrad)
172	$\Delta\theta_X$	15.0 ± 0.1	15.5 ± 0.1	13.5 ± 0.03	14.83 ± 0.03
	$\Delta\theta_Y$	15.3 ± 0.1	15.7 ± 0.1	13.5 ± 0.03	14.77 ± 0.03
200	$\Delta\theta_X$	13.1 ± 0.2	12.7 ± 0.2	14.4 ± 0.05	12.97 ± 0.04
	$\Delta\theta_Y$	12.9 ± 0.2	12.8 ± 0.2	14.3 ± 0.05	12.84 ± 0.04
240	$\Delta\theta_X$	10.9 ± 0.1	10.6 ± 0.1	11.5 ± 0.03	10.84 ± 0.03
	$\Delta\theta_Y$	10.9 ± 0.1	10.9 ± 0.1	11.5 ± 0.03	10.83 ± 0.03
p		$\langle\theta_{Scatt}\rangle_{G4}^{meas}$ (mr)	$\langle\theta_{Scatt}\rangle_{CC}^{meas}$ (mr)	$\langle\theta_{Scatt}\rangle_{G4}^{model}$ (mr)	$\langle\theta_{Scatt}\rangle_{CC}^{model}$ (mr)
172		20.3 ± 0.2	20.4 ± 0.2	17.7 ± 0.03	19.1 ± 0.03
200		17.1 ± 0.2	16.4 ± 0.2	19.1 ± 0.05	16.5 ± 0.04
240		13.8 ± 0.1	13.7 ± 0.1	15.0 ± 0.03	13.7 ± 0.03

measurements from the pseudo-experiments

The MICE super conducting magnets are to be operated together for the first time in the fall of 2016. At that time the program of scattering in LiH will be resumed with the magnetic fields on. This program has a few advantages; the first is that muons at angles greater than 35 mrad clip elements of the channel when the field is off. This clipping is not optimal as fiducial angles should be greater than 2σ of the raw scattering distribution. With the fields on, larger angles are contained so the acceptance of the apparatus should increase. Similar selection criteria should apply to the field off and field on analyses, so a similar analysis methods should be applicable with a few exceptions. The analysis will require extrapolation to the absorber to determine the initial and final angles in the absorber material. With a larger set of initial angles there is the potential for measurements with different effective absorber thicknesses. Initial studies are now under way.

5 Conclusions

Multiple scattering is a well understood phenomenon, but there are some inconsistencies between data and simulation. Particularly, simulations in GEANT4 have not matched the data well for muons in low Z materials. Data have been collected to validate the simulation for MICE specifically with muon beams at three different momentum settings using an empty channel and a lithium hydride absorber. Other absorbers have been used in the past; specifically scattering data with a vessel containing Xenon gas have been collected but the analysis has not been presented here; and a liquid hydrogen absorber will be used in the future. Average projected scattering widths from 65 mm of LiH have been measured to be 15.6 ± 0.1 mrad at 172 MeV/c, 12.8 ± 0.2 mrad at 200 MeV/c and 10.8 ± 0.1 mrad at 240 MeV/c. Studies of the systematics affecting these measurements are still in progress.

The work described here was made possible by grants from U.S. DOE and NSF, Italian INFN, U.K. SFTC, the European Community under the European Commission Framework Programme 7, The Japan Society for the Promotion of Science and the Swiss National Science Foundation. We are grateful to the staff of ISIS for its reliable operation. We acknowledge the use of Grid computing resources deployed and operated by GridPP in the UK. <http://www.gridpp.ac.uk/>.

6 References

1. D. Adams et al. Characterisation of the muon beams for the Muon Ionisation Cooling Experiment. *Eur. Phys. J.*, C73(10):2582, 2013.
2. M. Bogomilov, R. Matev, R. Tsenov, M. Dracos, M. Bonesini, et al. Neutrino factory. *Phys.Rev.ST Accel.Beams*, 17(12):121002, 2014.
3. Diktys Stratakis and Robert B. Palmer. Rectilinear six-dimensional ionization cooling channel for a muon collider: A theoretical and numerical study. *Phys. Rev. ST Accel. Beams*, 18:031003, Mar 2015.
4. Bruno Rossi and Kenneth Greisen. Cosmic-ray theory. *Rev. Mod. Phys.*, 13:240–309, 1941.
5. D. Attwood et al. The scattering of muons in low Z materials. *Nucl. Instrum. Meth.*, B251:41–55, 2006.
6. Timothy Carlisle. *Step IV of the Muon Ionization Cooling Experiment (MICE) and the multiple scattering of muons*. PhD thesis, Oxford U., 2013.
7. G. D’Agostini. A Multidimensional unfolding method based on Bayes’ theorem. *Nucl. Instrum. Meth.*, A362:487–498, 1995.
8. Tim Adye. Unfolding algorithms and tests using RooUnfold. In *Proceedings of the PHYSTAT 2011 Workshop, CERN, Geneva, Switzerland, January 2011, CERN-2011-006, pp 313-318*, pages 313–318, 2011.